Performance Improvement of Spark-Ignited Medium Speed Gas Engine 28AGS

NAKAYAMA Sadao : Research & Development Department, Engineering & Technology Center, IHI Power Systems Co., Ltd.
KUROIWA Takanori : Research & Development Department, Engineering & Technology Center, IHI Power Systems Co., Ltd.
NAKAZATO Takafumi : Research & Development Department, Engineering & Technology Center, IHI Power Systems Co., Ltd.
SAITO Toshiyuki : P. E. Jp (Mech), General Manager, Injection System Design Group, NICO Precision Co., Inc.

Gas engines are environmentally-friendly due to their clean exhaust, and the markets for both land power generation facilities and the marine sector are expanding. In line with the demand in these markets, IHI Power Systems Co., Ltd. has manufactured and installed economically-efficient, environmentally-friendly, safe gas-fueled engines for over 30 years. Utilizing the technical insights that we gained in past development work, increasing the efficiency of gas engines for power generation was set as a next development target. The development work was carried out based on NIIGATA high-efficiency gas engine 28AGS developed in 2012. This paper describes the research and development of the higher-efficiency gas engine.

1. Introduction

Gas engines are environmentally-friendly because their exhaust gases are clean, and the gas engine market is expanding not only in the field of power generation facilities on land but also in the field of marine use. In response to these market requirements, IHI Power Systems Co., Ltd. (IPS) has produced and delivered large gas engines that pursue environmental feasibility and safety in addition to cost efficiency. We have set the next development target to further improve the efficiency of power generation gas engines by utilizing our technical knowledge accumulated to date. The engine used as the basis of development is the NIIGATA 28AGS, a spark-ignited lean-burn gas engine. This paper describes development of several underlying technologies for the high-efficiency gas engine.

2. History of NIIGATA gas engine development

IPS has produced and delivered gas engines for more than 30 years in response to market demand. Based on the highly reliable PA5 diesel engine, IPS has developed dual-fuel engines that can be run by both liquid fuel and gas fuel and then spark-ignited lean-burn gas engines 26HX-G and 33CX-G. **Figure 1** illustrates the history of NIIGATA gas engine development. The 28AHX-DF dual-fuel engine for ship propulsion, which is the world's first FPP (Fixed Pitch Propeller) direct drive application developed to comply with the environmental regulations that are becoming strict in marine field in particular, has been favorably evaluated because of its high performance and stability. Moreover, the micro-pilot gas engine that has been on the market since 2002 is highly valued by many customers because it maintains high performance and remains superior in cost efficiency even today. In 2012, we completed development of the NIIGATA 28AGS, whose high performance is further improved by a spark ignition system, and this engine is now commercially available.

3. Market environment

3.1 Land sector

In Japan, there are an increasing number of cases in which co-generation systems are used as part of measures for BCP (Business Continuity Planning) because of the experience of the Great East Japan Earthquake in 2011. In particular, for plants that use a lot of electricity, electric power shortages greatly impact productivity. Therefore, introduction of gas engine co-generation systems at these plants to serve as non-utility power generation facilities is underway. Moreover, communities and industrial parks have begun cooperating with each other to introduce systems to efficiently supply energy to their facilities while controlling and promoting optimization of the energy (electricity and heat) generated by non-utility power generation facilities and the electricity purchased from electric power companies.

Meanwhile, gas fuels are also attracting much attention worldwide because of increased use of the new energy source as shale gas. Though shale gas is a fossil fuel, its minable years have been significantly extended by technological innovation. Moreover, because of the difference in price between liquid fuel and gas fuel, gas engines have reasonable cost efficiency in some cases. Thus, expectations

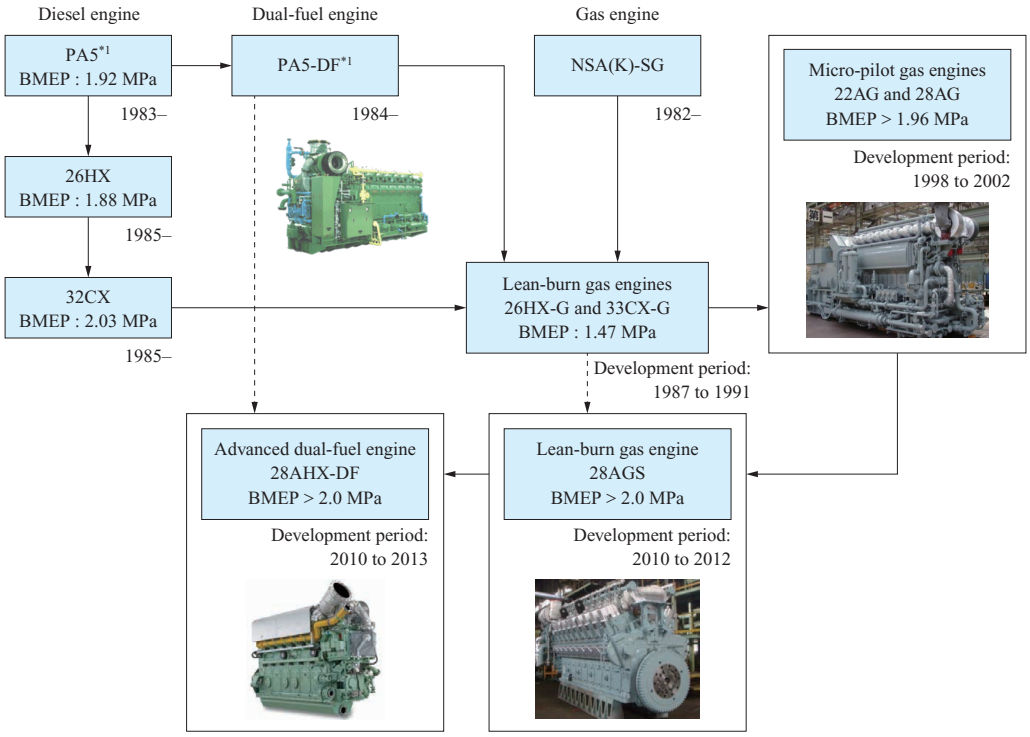

(Notes) BMEP : Brake Mean Effective Pressure
*1 : Jointly developed with S.E.M.T (the present MAN Diesel SAS of France)

Fig. 1 History of NIIGATA gas engine development

for gas engines are increasing.

3.2 Marine sector

As represented by the IMO (International Maritime Organization) NO_x Tier III regulations, environmental regulations for ships are becoming increasingly strict year after year. In the case of diesel engines, it is difficult to satisfy such regulations with the engines alone, so the exhaust gases are cleaned by additional denitrification equipment such as an SCR (Selective Catalytic Reduction) system. However, given the small space available on ships, there may be problems such as the difficulty of securing installation space and increase in cost.

Figure 2[1] shows a comparison of the harmful exhaust gas components categorized based on the differences among fuel types. In the case of gas engines, NO_x emissions can be reduced compared to diesel engines through lean combustion, in addition to the fact that small amount of harmful substances is derived from gas fuels (**Fig. 2**). Therefore, it is possible to satisfy emission regulations with only the engine without additional equipment such as an SCR system. However, to use gas engines for ship propulsion, problems remain to be solved with regard to dynamic characteristics. Thus, in the case of gas engines for ship propulsion, besides improving engine performance, hybrid systems that combine electric propulsion systems with power storage devices are also adopted in some cases.

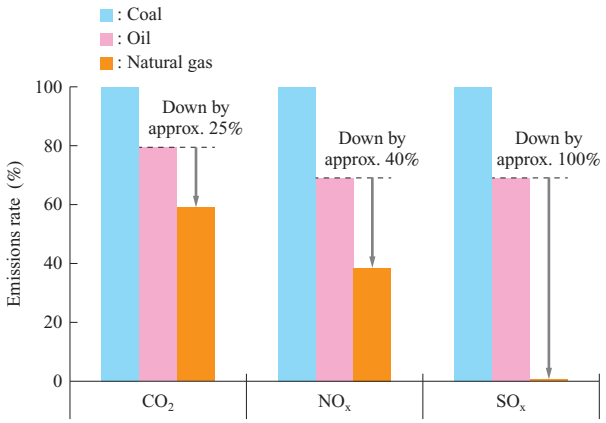

Fig. 2 Comparison of the harmful exhaust gas components categorized based on the differences among fuel types

4. Development process

4.1 Development target

Table 1[2] shows the specifications and lineup of the 28AGS engine, which was the basis of the development. This engine is a spark-ignited lean-burn gas engine that ignites an air-fuel mixture of theoretical air-fuel ratio in the PCC (Pre-Combustion Chamber) with a spark plug and that makes the flame jets from the PCC burn a lean mixture in the MCC (Main Combustion Chamber). The lineup ranges from 6L to 18V cylinder, covering an output range of 2 to 6 MW. By applying the newest spark ignition technology to the micro-pilot engines 22AG and 28AG, which have a track record of more than 100 engines delivered and operated, high power generation efficiency is achieved while keeping NO_x emissions low. Among these engines, in-line engine with 2 MW-power output achieved the world's highest level of power generation efficiency at the time. The 28AGS has

Table 1 28AGS specifications

Item		Unit	Specifications				
Number and arrangement of cylinders		—	6L	8L	12V	16V	18V
Bore		mm	295				
Stroke		mm	400				
Rotational speed		min^{-1}	750/720				
Generator output	50 Hz	kW	2 000	2 650	4 000	5 300	6 000
	60 Hz	kW	1 900	2 550	3 800	5 100	5 750
Brake mean effective pressure		MPa	2.0				
Ignition method		—	Spark ignition				
Combustion method		—	PCC (Pre-Combustion Chamber)				
Starting method		—	Air starter				
Fuel type		—	Natural gas, LNG				

(Notes) Site conditions: ISO 15550, Generator power factor: 0.9, Fuel gas lower heating value: 40.6 MJ/m^3N, Methane number: 65 or higher

sufficient load response characteristics achieved by optimized air-fuel ratio control[3]. Moreover, it has received much attention as a BCP measure after the Great East Japan Earthquake because of its two functions: function for important load survival operation and function for a power generation system for both emergency and regular use. The important load survival operation means that in the case of an outage in the connected commercial power supply during transmission, the power generation equipment instantaneously disconnects from the commercial power supply and continues operation to supply power only to the important loads. The 28AGS can be used as a power generation system for both emergency and regular use because it can establish its voltage within 40 seconds from startup. Even after the release of the 28AGS Series, the continuous improvement in the performance was important to enhance the competitiveness of NIIGATA gas engines.

In this development, we decided to promote our efforts step-by-step in order to achieve the development target values listed in **Table 2**, while maintaining the superior characteristics of the 28AGS. Development for Step 1 was already completed, and we have been engaged in Step 2.

4.2 Development concept

The following factors were reviewed as a means of improving efficiency to achieve the targets of Step 1 listed in **Table 2**.

4.2.1 Stabilization of combustion in the PCC by strengthening ignition source

(1) Improvement of combustion by stabilizing and strengthening the flame jets from the PCC to the MCC

The schematic of the combustion chamber is shown in **Fig. 3**. In the case of a spark ignition system that is equipped with the 28AGS, a spark discharged from the spark plug is used as the ignition source. This causes the burning of the air-fuel mixture which is very close to the theoretical air-fuel ratio. Then, the lean mixture in the MCC burns by a flame jet from the PCC. Thus, to achieve stable combustion of lean mixture in the MCC, it is absolutely necessary to stabilize the flame jets generated in the PCC. Therefore, as the first step, we focused on optimization of the flow conditions and the gas concentration distribution around the spark plug by changing the shape of the PCC.

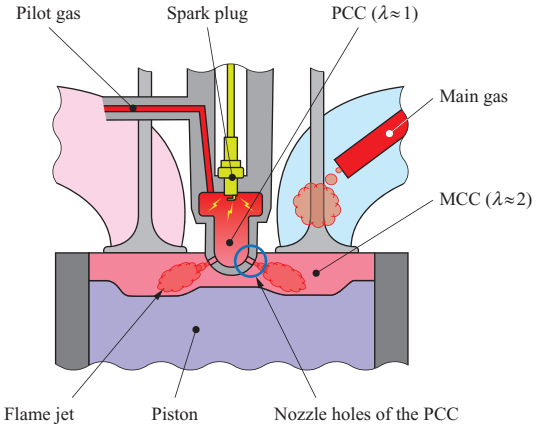

Fig. 3 Schematic of the combustion chamber

(2) Reduction of unburned gas fuel (methane slip)

Next, reducing the discharge of unburned gas fuel is a means of improving environmental feasibility, not just power generation efficiency. In the case of the 28AGS, gas fuel is injected by a solenoid valve installed in each cylinder, and the gas fuel is mixed with air in the intake port and then supplied to the MCC. The lean mixture that flowed into many crevices in the MCC does not burn due to excessive heat loss at the wall of the MCC, and it is discharged as a greenhouse gas (methane slip). Therefore, we decided to reduce the portion that can remain unburned (hereinafter referred to as the "dead volume").

(3) Knocking suppression by homogenizing the air-fuel mixture

As gas fuel must be supplied to the MCC while

Table 2 Development target

Item		Development target				
Number and arrangement of cylinders		6L	8L	12V	16V	18V
Electrical efficiency (%) (with a tolerance of 5%)	Base	45.5	45.7	47.0	47.2	47.4
	Step 1	47.8	48.0	49.3	49.7	49.9
	Step 2	Step 1 + 1.0%pt				

(Notes) Site conditions: ISO 15550, Generator power factor: 0.9, Fuel gas lower heating value: 40.6 MJ/m^3N, Methane number: 65 or higher

intake valve is open, the solenoid valve must inject it quickly. Moreover, because there is a difference in the length of the flow channel from the solenoid valve for gas fuel supply to the two intake valves, the concentration distribution of the mixture in the MCC tends to be uneven. During combustion, this unevenness of mixture concentration can cause variation in flame propagation speed and knocking. Therefore, we used 3D-CFD (Computational Fluid Dynamics) simulation to review the shape of the gas nozzle in the lower part of the solenoid valve, and we attempted to equalize the mixture concentration in the MCC.

4.2.2 Ensuring combustion stability by optimizing air-fuel ratio control

As factors necessary for stable combustion, we focused on two points: air-fuel ratio control and balance control between cylinders. The 28AGS uses an intake air bypass system, which returns the air compressed by the turbocharger's compressor to the upstream of the compressor. The air-fuel ratio is controlled within an appropriate range with the bypass valve to control the volume of air that passes through this bypass line. This system offers the advantage of using the bypass valve at relatively low temperatures. On the other hand, the compression energy for the air to be returned to the upstream of the compressor is an inefficient task for the turbocharger, and it disadvantageously reduces the turbocharging system's overall efficiency. Therefore, we focused on the wastegate system, which has a bypass line on the turbocharger's turbine side. In the wastegate system, as exhaust gas is discharged from the bypass line to the downstream of the turbine, the pressure of exhaust manifold falls, and the pumping loss in the exhaust stroke can be reduced. Moreover, as this makes it possible to increase the differential pressure between the intake and exhaust, there is the advantage of improved cylinder charging efficiency. As for control of the balance between cylinders, we introduced a method to precisely control ignition timing and air-fuel ratio of each cylinder while monitoring the combustion using the in-cylinder pressure sensor.

4.2.3 Reduction of mechanical loss and cooling loss

We also started efforts to reduce energy loss. One such effort was to reduce mechanical loss, such as the friction of piston rings and bearings. To reduce mechanical loss, it is effective to reduce the viscosity of the lubricating oil. Therefore, while reviewing the engine design, we considered the allowable minimum viscosity of lubricating oil. We achieved appropriate viscosity by adjusting the temperature of lubricating oil. The other effort was to reduce heat loss of the cooling water. We reduced cooling loss by raising the temperature by the cooling water of the engine. However, as the combustion chamber's wall temperature rises in response to the rise in cooling water temperature, abnormal combustion (e.g., knocking) tends to occur due to overheating of unburned gas. Therefore, knocking suppression technology as described in **Section 4.2.1 (3)** must be used in combination.

In **Chapter 5**, we will discuss optimization of the PCC shape and dead volume reduction, which greatly contributed to efficiency improvement.

5. Development of underlying technology for efficiency improvement

5.1 Optimization of the shape of the PCC

As described above, the air-fuel mixture in the PCC immediately before ignition is macroscopically stoichiometric, but its local concentration tends to be uneven. Hence, unless ignition and combustion in the PCC are stabilized, the flame jets issued into the MCC vary between cycles, adversely impacting combustion stability in the MCC. Therefore, to reinforce the ignition source for the MCC, we addressed to improve combustion stabilization in the PCC based on the combustion improvement logics of the PCC and that of the MCC as shown in **Fig. 4**.

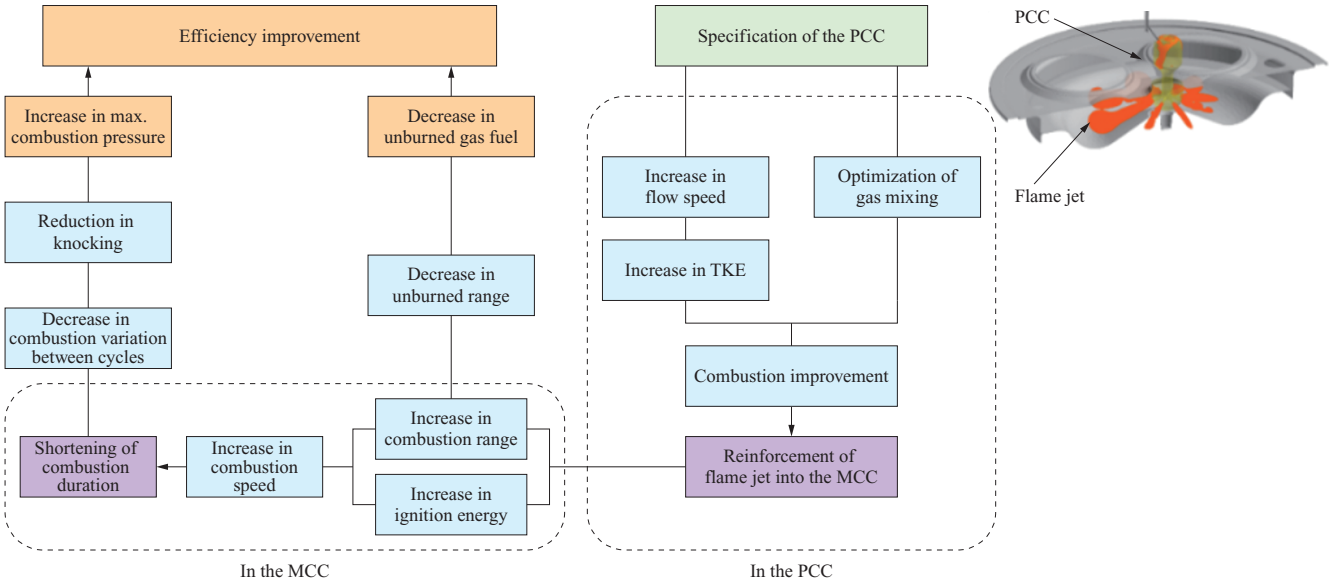

Fig. 4 Logic of improving combustion in Pre-Combustion Chamber (PCC) and Main Combustion Chamber (MCC)

The calculation parameters for the shape of the PCC are shown in **Fig. 5**. The shape of each part of the PCC (**Fig. 5-(a)**) was used as a calculation parameter, and 3D-CFD simulation was conducted on the combination conditions of **-(b)**[4]. For the evaluation parameter, TKE (Turbulent Kinetic Energy) in the PCC was mainly used.

Figure 6 shows the relationship between V2/V1 and TKE, while **Fig. 7** shows the relationship between the total area of nozzle holes and TKE. Among the calculation parameters of the PCC, the representative factors that had a great impact on the increase in TKE were the volume ratio V2/V1 (**Fig. 6**) of V2 (the main body of PCC) and V1 (throat part) as well as the total area of the nozzle holes (**Fig. 7**). The flow in V2 is generated by the flow of gas fuel injected from the gas fuel supply channel above V2 and the flow of lean mixture that has flowed in from the MCC. Based on these results, it can be considered that narrowing the flow path through which the lean mixture flows from the MCC makes higher flow velocity in the PCC and increased TKE.

Increased TKE promotes combustion in the PCC and results in higher combustion pressure in the PCC. **Figure 8** shows the relationship between TKE and the combustion pressure (ΔP_{max}) in the PCC. As for the combustion pressure in the PCC under discussion here, the differential pressure (ΔP_{max}) between the maximum combustion pressure (P2) in the PCC and the pressure (P1) in the MCC immediately after ignition by the spark plug was used as an index. **Figure 9** shows the evaluation index of ΔP_{max} : TKE; **Fig. 10** shows the rate of heat release in the PCC; and **Fig. 11** shows the MFB (Mass Fraction Burned) in the PCC. The increase in ΔP_{max} is caused by the accelerated combustion in the PCC due to the increase in TKE. The rate of heat release in the PCC increased faster (**Fig. 10**) and the MFB reached 50% level faster after optimization even though the ignition timing was the same.

Also, the rise in ΔP_{max} is an increase in the energy of the flame jets issued from the PCC into the MCC, which means that the ignition source for the lean mixture in the MCC was strengthened. **Figure 12** shows the combustion pressure in

(a) Shape of the PCC

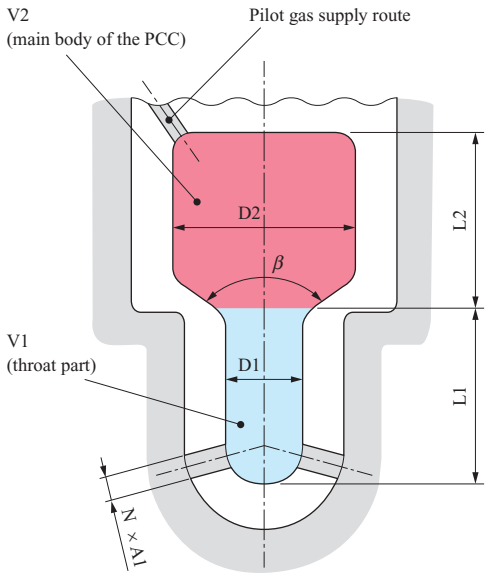

(b) Combination conditions of calculation parameters

No.	Inner diameter		Length		Volume		Total area of the nozzle holes	Throat angle
	(D1)	(D2)	(L1)	(L2)	(V1)	(V2)	(N × A1)	(β)
Base	1.00	1.00	1.00	1.00	1.00	1.00	1.00	1.0
Case 1	0.73	1.00	1.00	1.15	0.53	1.09	0.25	1.0
Case 2	0.73	1.00	1.00	1.15	0.54	1.09	0.25	1.0
Case 3	0.80	1.00	1.00	1.11	0.65	1.07	0.34	1.0
Case 4	0.90	1.00	1.00	1.05	0.82	1.04	0.49	1.0
Case 5	0.73	1.00	1.00	1.00	0.55	1.09	0.25	1.5
Case 6	1.00	1.00	1.00	1.00	1.00	1.00	0.55	1.0
Case 7	0.73	0.75	0.91	0.93	0.49	0.73	0.25	1.5
Case 8	0.80	0.75	0.91	1.00	0.59	0.70	0.34	1.5
Case 9	0.73	0.75	0.91	0.93	0.49	0.73	0.25	1.5
Case 10	0.73	0.75	0.91	0.85	0.49	0.57	0.25	1.5
Case 11	0.73	0.75	0.91	1.02	0.49	0.73	0.25	1.0
Case 12	1.00	0.75	0.91	0.86	0.49	0.73	0.25	1.5
Case 13	0.73	0.75	0.91	0.93	0.49	0.73	0.25	1.5
Case 14	0.73	0.75	0.91	0.88	0.49	0.73	0.21	1.5
Case 15	0.73	0.75	0.91	0.88	0.49	0.73	0.16	1.5

(Note) Each value indicates the ratio to the PCC as a base.

Fig. 5 Parameters for PCC shape

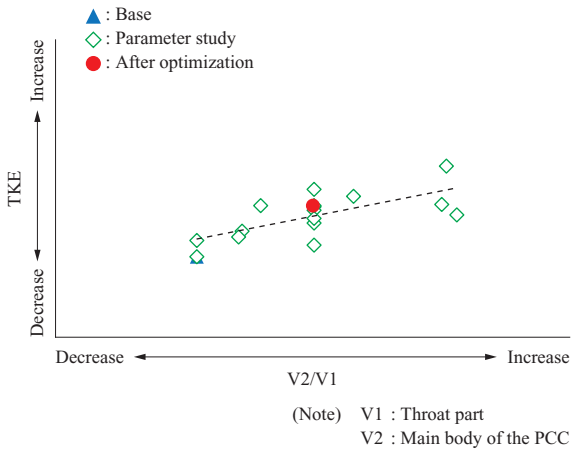

(Note) V1 : Throat part
V2 : Main body of the PCC

Fig. 6 Relationship between TKE and V2/V1

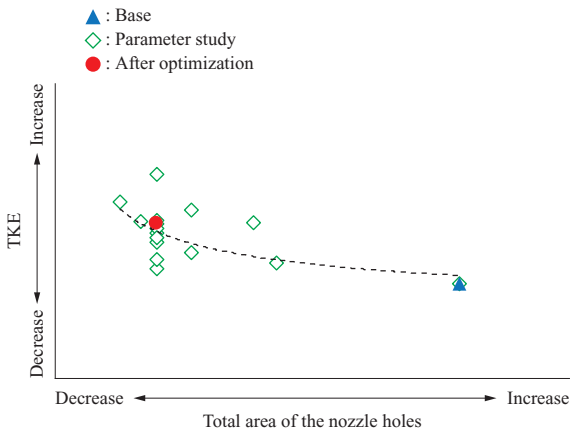

Fig. 7 Relationship between TKE and total area of nozzle holes

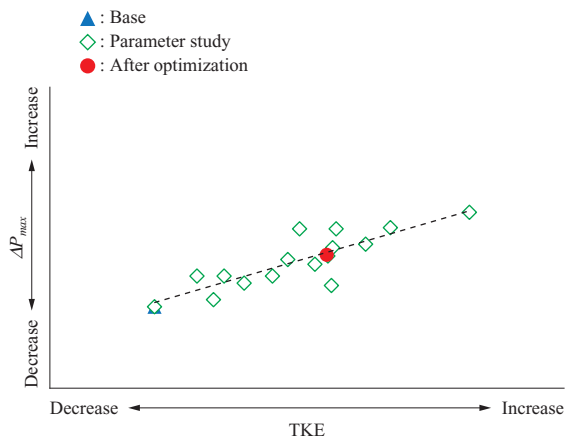

Fig. 8 Relationship between ΔP_{max} and TKE

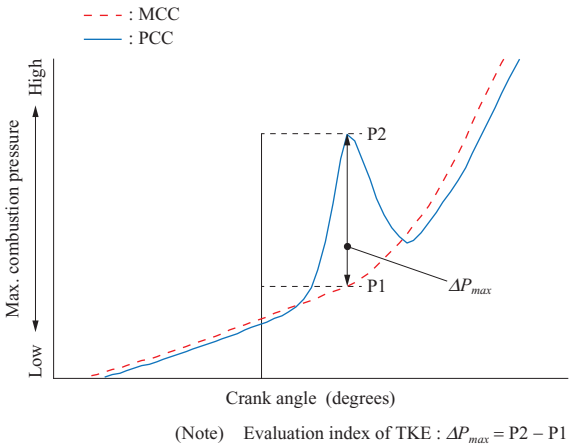

(Note) Evaluation index of TKE : ΔP_{max} = P2 – P1

Fig. 9 ΔP_{max} : Evaluation index for TKE

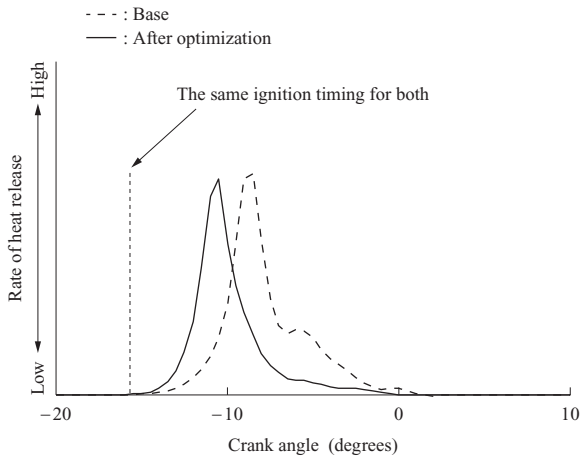

Fig. 10 Rate of heat release in PCC

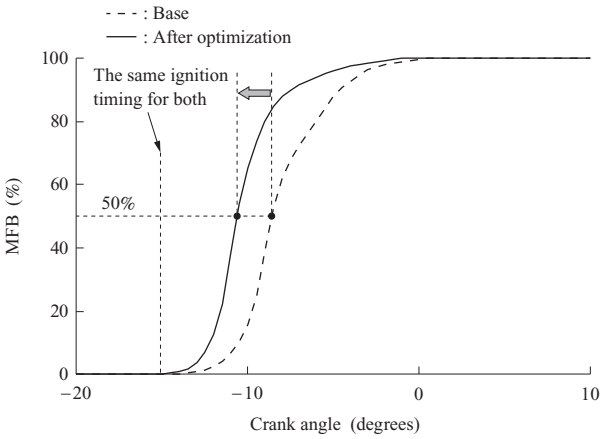

Fig. 11 Mass fraction burned in PCC

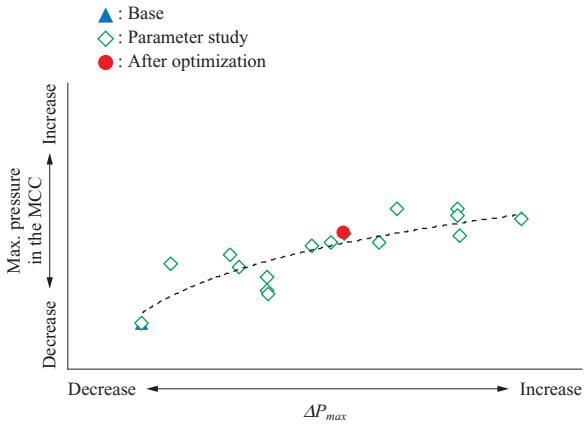

Fig. 12 Peak firing pressure in MCC

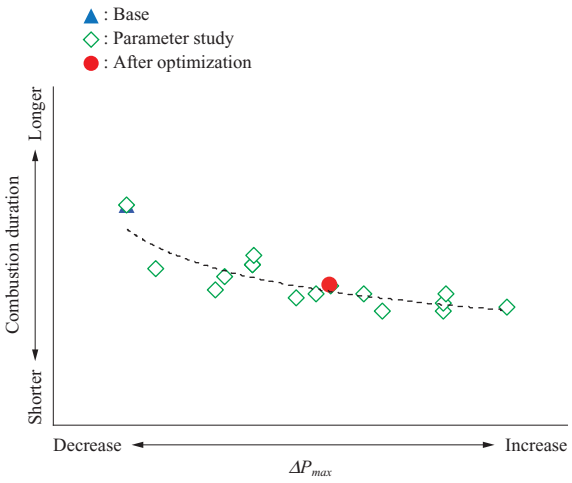

Fig. 13 Duration of combustion in MCC

the MCC, while **Fig. 13** shows the combustion duration of the MCC. As a result, the maximum combustion pressure in the MCC also increased (**Fig. 12**), and the combustion duration was shortened (**Fig. 13**). It is also expected that the flame jet variation among cycles will be reduced. However, because excessive reinforcement of ignition sources may cause higher combustion pressure than the allowable values and increase NO_x, we decided upon an appropriate shape for the PCC after considering margins to address this issue.

As a result of verification by the 6L test engine, it was confirmed that combustion variation in the MCC could be reduced. **Figure 14** shows the trends for the maximum combustion pressure in the MCC before and after the shape of the PCC was optimized. The COV (Coefficient Of Variation) between cycles was improved by approximately 20%. The combustion pressure in the MCC could be kept

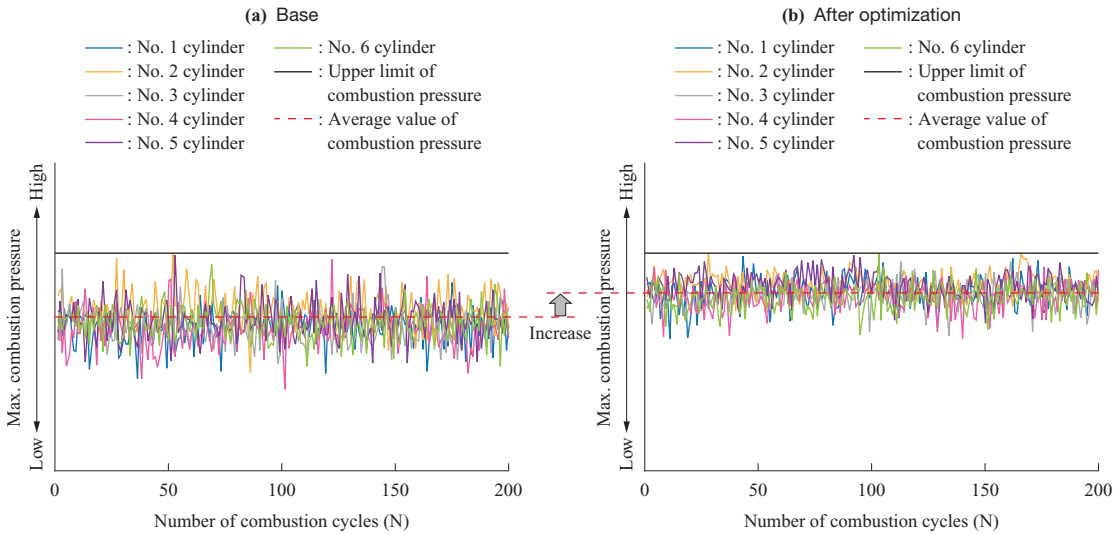

Fig. 14 PFP trends — Before and after optimization

high without exceeding the upper limit of combustion pressure as shown in **Fig. 15**, which indicates the variation range of maximum combustion pressure in the MCC. As a result, thermal efficiency was improved by approximately 0.4%pt.

5.2 Reduction of dead volume

Reducing the dead volume achieves two effects: improved efficiency by reducing unnecessary supply of gas fuel and reduction of methane slip emissions[5]. Moreover, because the air-fuel mixture that flowed into the dead volume part flows out to the combustion area in the expansion stroke, it can cause unusual combustion (e.g., knocking). In this way, dead volume reduction contributes to improve combustion stability in addition to improve performance and, to reduce environmental loads.

We closely examined the dead volumes in combustion chambers and considered how to reduce them. There are multiple (large and small) dead volumes in combustion chambers as shown in **Fig. 16**. Among these, in areas of particularly large volume, there are gaps (top land part) between the piston and cylinder liner as well as gaps (labyrinth part) between the cylinder head and cylinder liner (the portions indicated by dashed lines in **Fig. 16**). In the top land part, it is effective to reduce the volume by raising the position of the piston top ring. However, if the position of top ring groove is raised too high, it becomes difficult to form oil galleries for cooling the piston head. As a result, parts cannot be cooled sufficiently, and lubricating oil carbonizes, leading to locking of the piston rings and damage to sliding parts. Moreover, local heat spots at the piston head may cause knocking.

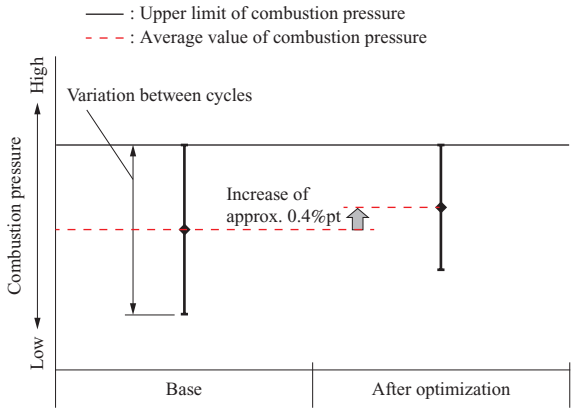

Fig. 15 Variation of maximum combustion pressure in the MCC

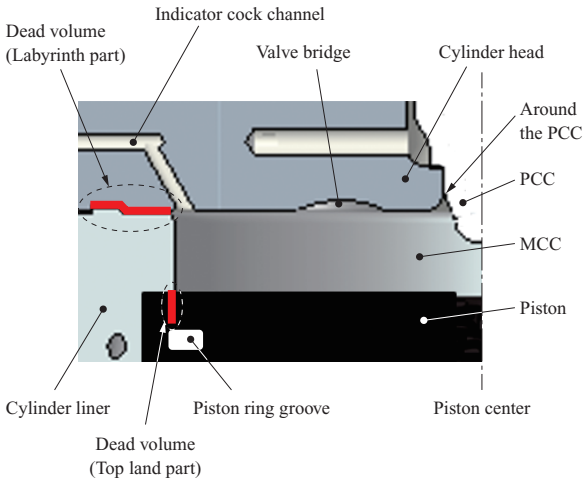

Fig. 16 Dead volume areas inside the combustion chamber

Therefore, with the top land volume in the early stages of development of the 28AGS base engine as a reference, we changed the position of the piston top ring and conducted tests on the changes in top land volumes. The top land volume and the temperature of the piston top ring groove are shown in **Fig. 17**. Even though the top land volume was reduced by approximately 40% compared to the reference, there were no large changes in temperature of the piston top ring groove. However, when the top land volume was reduced by approximately 80%, the temperature rose and reached the level at which the probability of lubricating oil carbonization increases. Based on these results, we determined a piston top ring position where dead volumes can be reduced and the

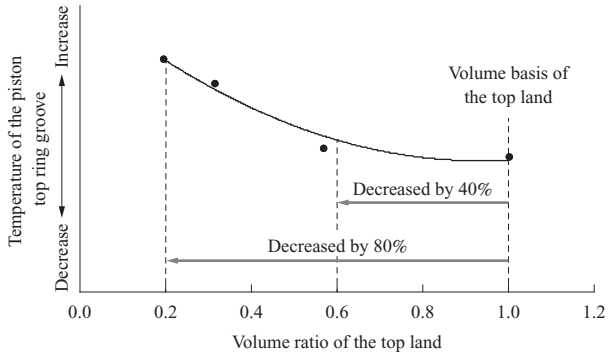

Fig. 17 Temperature measurement results at piston ring groove

temperatures of the piston and piston ring will not rise too much.

These efforts reduced dead volumes by approximately 50% and unburned gas fuel by approximately 40% compared to the 28AGS base engine.

5.3 Combination of underlying technologies and field evaluation

With the combination of the methods described in **Sections 5.1 and 5.2** and the underlying technologies described in **Section 4.2**, it was confirmed that the 6L test unit achieved Step 1's target value of an approximately 2.3% efficiency improvement. Some of the underlying technologies have already been applied in the field and evaluated. However, some elements related to durability that require many hours for evaluation (e.g., spark plugs) have not yet been fully verified. Such spark plugs are operated under various conditions at the sites, and track records of 5 000 or more hours of continuous operation have been achieved. We will continue to verify and evaluate the reliability (durability) through continuous operation. **Figure 18** shows an example evaluation of spark plug service life in the field.

6. Further improvement of power generation efficiency

We have completed development for Step 1, and we are currently working on to achieve Step 2. In Step 2, we focused on the following factors while reviewing the factors from Step 1.

(1) Stabilization of combustion in the PCC by reinforcement of spark ignition sources (advancement of Step 1)

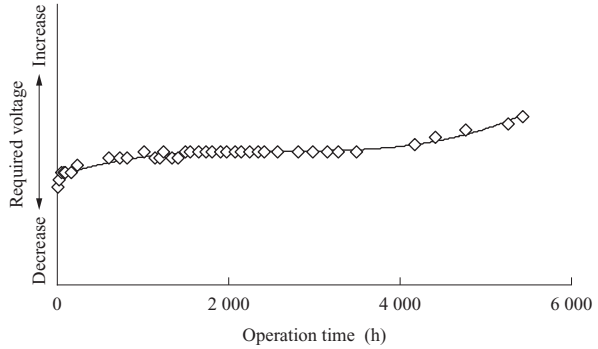

Fig. 18 Field evaluation of the spark plug

(2) Turbocharging efficiency improvement by valve overlap optimization

(3) Pumping loss reduction by reducing pressure loss of the intake air

First, we reviewed the shape of the PCC that was optimized in Step 1 and promoted further improvement. In Step 2, as a result, we achieved higher combustion stability than Step 1, and the COV decreased by approximately 50% compared to the base (**Fig. 14-(a)**). **Figure 19** shows the trend in maximum combustion pressure in the MCC after optimization in Step 2. Further efficiency improvement can be expected by adopting an earlier Intake Valve Closing (IVC) timing (stronger Miller) and increased compression ratio.

As abnormal combustion (e.g., preignition and knocking) can be reduced by decreasing the compression end temperature, decreasing the effective compression ratio by stronger Miller is effective. Together with this, the cycle efficiency can also be improved simultaneously by increasing the expansion ratio while optimizing the geometric compression ratio. However, to fully achieve these effects, combustion must be stabilized by means of high turbocharging efficiency and further reinforcement of ignition sources.

Figure 20 shows an example analysis with one-dimensional simulation of the IVC timing. With the IVC timing at the time of Step 1 as the base, we conducted parameter studies

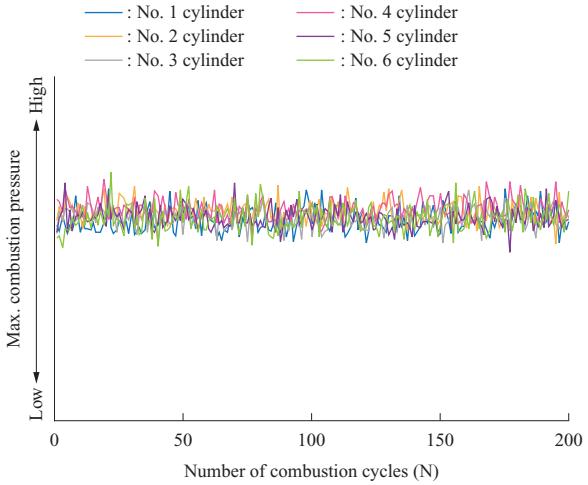

Fig. 19 PFP trends — After re-optimization (Step 2)

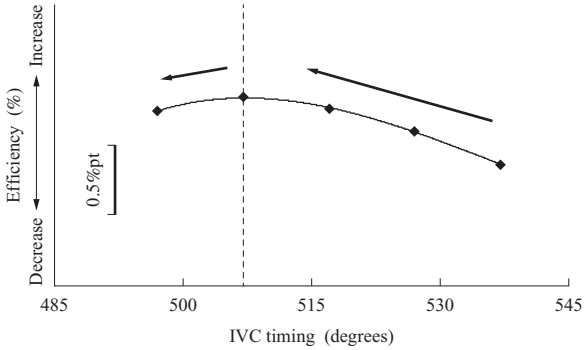

Fig. 20 Example of the 1D simulation result

and narrowed down the candidate timings. If the IVC timing is advanced beyond a certain extent, the amount of pumping loss increases with the decrease in effective compression ratio, leading to decreased efficiency as shown in **Fig. 20**. Based on this result, we selected the IVC timing that achieves the highest efficiency.

In addition, we also reviewed the valve overlap with one-dimensional simulation. **Figure 21** shows a typical example of valve lift in the case in which the valve overlap is changed by changing the EVC (Exhaust Valve Closing) timing. By decreasing valve overlap, it is possible to reduce the outflow of unburned gas fuel during valve overlap and to increase thermal efficiency. **Figure 22** shows the effect of changing the valve overlap. On the other hand, shortening the valve overlap reduces the cylinder charging efficiency. As a result, the ratio of burned gas remaining in the combustion chamber increases, and the amount of fresh air to be used in the next cycle of combustion decreases. This means that the pressure difference between intake and exhaust decreased, which deteriorates transient performance. Therefore, we attempted to optimize the valve timing and geometric compression ratio while considering these advantages and disadvantages. We confirmed that the final combination improved efficiency by approximately 0.2%pt with the 6L test engine.

Moreover, to ensure the necessary air quantity with stronger Miller timing, boost pressure should further be increased. As a result, the pressure loss of the intake air increases, and the turbocharging efficiency decreases. As the factors to be added to the effects of efficiency improvement by optimization of the aforesaid valve timing and geometric compression ratio, we also attempt to reduce pressure loss of the intake air with the aim of reducing pumping loss.

The pressure loss of the intake air is largely affected by the shapes of the intake runner and intake valve. As a result of analyses with 3D-CFD, we found separation of flow near the port wall and around the intake valve. To reduce the pressure loss due to the separation, we fine-tuned the shape of the flow channel. To improve the air-gas mixture as well, we also reviewed the shape of the gas nozzle on the upper part of the intake port. **Figure 23** shows an example of 3D-CFD aimed at the pressure loss of the intake air.

As a result of optimizing the shape of each part, the flow coefficient is estimated to improve by 10% or more. At present, we are producing parts for verification, and we are investigating the effects of reducing pressure loss in detail.

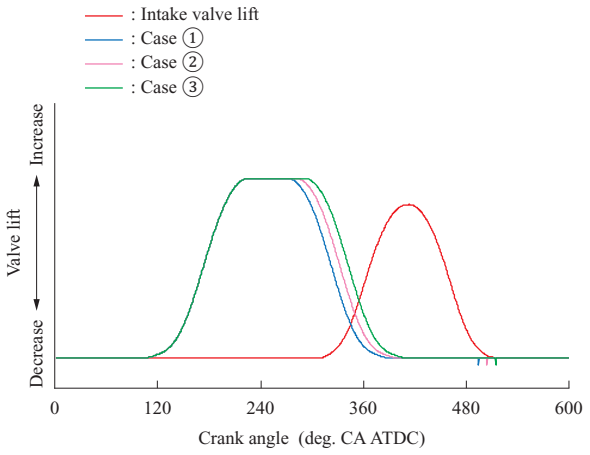

Fig. 21 Example of valve lift curves with the changed valve overlap

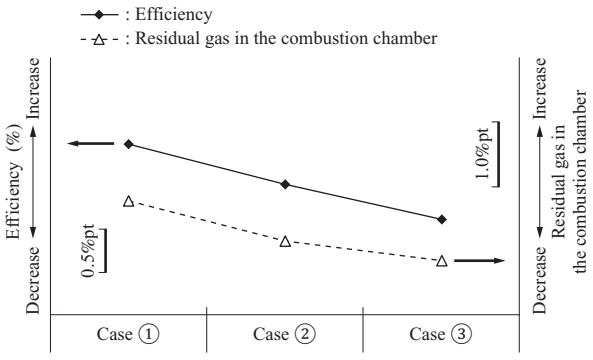

Fig. 22 Effects of the changed overlap

7. Conclusion

We have promoted the development of underlying technologies with the aim of achieving higher efficiency for the 28AGS power generation gas engine, which was developed in 2012. We have introduced various technologies, including improved combustion stability and reduced emissions from unburned gas fuel. As a result, in 2017, we released a product whose power generation efficiency has been increased by 2.3%pt compared to the base engine. At present, we are promoting the development of underlying technologies with the aim of further increasing efficiency by 1.0%pt.

As the trends of BMEP of gas engine are increasing in recent years, we also confirmed that the technologies

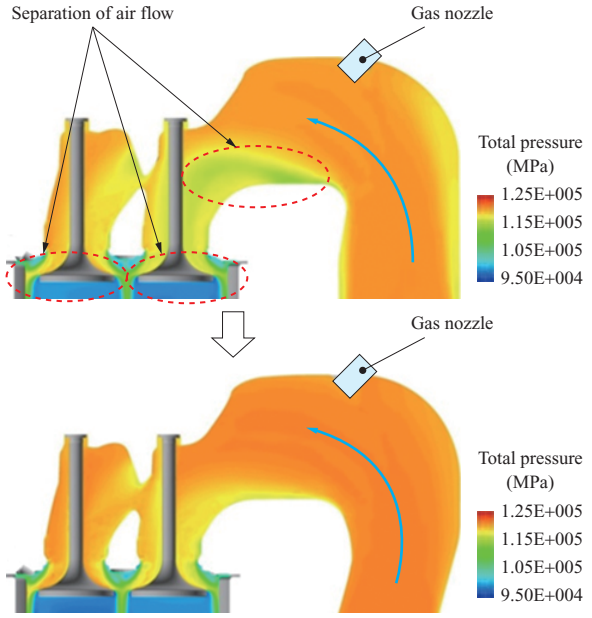

Fig. 23 3D-CFD result for reducing pressure loss of the intake air

acquired in this development are effective. We will continue to tackle further efficiency improvement and higher BMEP of gas engines as well as promote research and development to contribute to reducing CO_2 emissions, and we will provide products that meet market demands.

REFERENCES

(1) International Energy Agency (IEA) : Natural Gas Prospects to 2010, 1986

(2) K. Watanabe, S. Goto and T. Hashimoto : Advanced development of medium speed gas engine targeting to marine & land, 27th CIMAC World Congress on Combustion Engine Technology, Paper of CIMAC Congress 2013, 2013, No. 99

(3) S. Nakayama, S. Goto, T. Hashimoto and S. Takahashi : Experiences on 1 to 6 MW class highly adaptable micro-pilot gas engines in one hundred fields and over fifty thousand running hours, Paper of CIMAC Congress 2010, 2010, No. 125

(4) Z. Xu, T. Kuroiwa and J. Sato : The Latest Development of High Performance Gas Engine, The 6th TSME International Conference on Mechanical Engineering, Thai Society of Mechanical Engineering, 2015, No. AEC003

(5) The International Council on Combustion Engines (CIMAC) WG17, Gas Engines : Methane and Formaldehyde Emissions of Gas Engines, CIMAC Position paper, 2014, pp. 6-12